

X-Ray Photoconductive Nanocomposites

Ying Wang* and Norman Herron

The successful development of digital radiography depends, to a large extent, on the availability of suitable x-ray photoconductors. The x-ray photoconductive nanocomposites reported here combine the advantages of both inorganic and organic compounds. An inorganic compound was finely dispersed in an organic polymer. The inorganic compound, with its large x-ray absorption efficiency, functioned as the x-ray absorber, and the polymer provided good dielectric properties and ease of thin-film preparation. The preparation procedures and the x-ray photoconductive properties of a specific example, a 50 percent by weight nanocomposite of bismuth triiodide and nylon-11, are discussed in detail.

Nanocrystal and nanocomposite research represents an important emerging area in modern materials science (1-8). Nanocomposites are defined as composites in which one component has domain sizes smaller than tens of nanometers, down to the molecular size regime. The synergistic combination of inorganic and organic compounds in a nanocomposite not only can improve the existing material properties but also can create new functionalities that do not exist for either material alone. Here, we report the preparation and the x-ray photoconductive properties of nanocomposites consisting of bismuth triiodide (BiI_3) finely dispersed in nylon-11, $[-\text{NH}-\text{CO}-(\text{CH}_2)_{10}-]_n$. Neither BiI_3 nor nylon-11 alone shows such x-ray photoconductivity, which is one of the technologies being developed for digital radiography.

Radiography has been used for over 90 years to capture medical images (9). In conventional radiography, the x-ray image is captured on a flat sheet of phosphor material that emits light when stimulated by x-rays. The light emitted by the screen exposes a silver halide film that stores the image. This method is one of the major diagnostic tools in health care that is still in analog format, whereas, for example, magnetic resonance imaging and computed axial tomography are both "all-digital" techniques. Therefore, the development of digital radiography is highly desired and is being actively pursued.

One form of digital radiography currently under development uses x-ray-sensitive photoconductors (10-12). A useful x-ray photoconductive material must have the following properties. First, it must be a good insulator in the dark and must be capable of sustaining high electric fields (10^5 to 10^6 V cm^{-1}). Second, it must have a large x-ray

absorption cross section and high charge generation efficiency. Finally, the generated carriers must move through the film without significant trapping. In spite of many years of research, at present Se is the only useful x-ray photoconductive material that may meet these challenging requirements (10-13). It also has many drawbacks. The x-ray absorption efficiency of Se is not particularly high. Good-quality Se thin films, without carrier trapping sites, are notoriously difficult to prepare. The toxicity of Se and its safe handling are also of great concern.

There are several reasons why there are such difficulties associated with the development of new x-ray photoconductive materials. Although many heavy element-containing inorganic compounds such as BiI_3 absorb x-ray photons efficiently, it is difficult to fabricate them into large-area, good-quality thin films. Furthermore, they usually have high dark conductivity at room temperature and cannot sustain a large electric field. On the other hand, polymers can be fabricated into good-quality thin films, have low dark conductivity, and have good dielectric properties but are inefficient x-ray absorbers. The composite approach reported here combines the advantages of both the organic and inorganic compounds.

A number of criteria need to be met for this approach to work:

- 1) The composite should be a nanocomposite—that is, domain sizes should be very small. Mechanical mixing and the pressing together of large (micrometer-sized) inorganic particles and polymers has been shown to be ineffective. Such composites cannot support large electric fields and usually contain a large number of deep carrier traps (3, 14).

- 2) Because of the dilution effect of the polymer, the volume fraction of the inorganic component must be high enough to ensure that the total x-ray absorption remains strong. For example, in the case of

the BiI_3 -polymer, we have calculated that ~65% by weight BiI_3 is required in order for the x-ray absorption at 62 keV (tungsten radiation) of the composite to be comparable to that of Se. Such a large amount of inorganic compound must be dispersed into the polymer, while maintaining the polymer's mechanical and dielectric strength and yet avoiding the formation of carrier traps.

- 3) The composite must be a good electron or hole transport material. This may be achieved by the use of a carrier-transporting polymer such as *N*-polyvinylcarbazole or a polysilane (14). Alternatively, inorganic nanoparticles may percolate together to form a conducting pathway at high concentrations.

We have developed a number of inorganic-polymer nanocomposites that may fulfill these requirements, and we discuss the case of BiI_3 -nylon-11 in detail here. Bismuth triiodide is a layered material with octahedral coordination of the Bi (15). Intercalation or coordination chemistry can be used to exfoliate these layered materials into discrete molecular species (16), which allows the subsequent easy preparation of nanocomposites. We chose nylon for the production of these composites with BiI_3 because the polyamide moiety is very compatible with the known solubility properties of BiI_3 . The formation of Lewis base adducts of BiI_3 with amides, ethers, and S ligands is well documented (16), which accounts for the high solubility of BiI_3 as orange molecular coordination complexes in amide solvents. We found that BiI_3 at 50% by weight dissolved well in all polyamides we investigated (nylon-6; -6,6; -11; -12). This strong coordination of Bi with the amide linkages of the polymer (with consequent disruption of the polymer hydrogen-bonding network) may also explain the marked reduction in polymer melt viscosity that we have observed. Nylon-11 has a relatively low melting point (198°C) compared to that of other nylons, which allows relatively low-temperature processing and minimizes thermal degradation and oxidation.

We prepared the BiI_3 -nylon-11 nanocomposite by dissolving BiI_3 powder (from Alfa, Ward Hill, Massachusetts; 99.999% pure, Puratronic grade; recrystallized from tetrahydrofuran under N_2) in a melt of nylon-11 (previously dried under vacuum at 150°C to remove moisture) at 190° to 200°C under N_2 for 5 to 15 min to give a thick, clear orange solution. We made thick films (from hundreds of micrometers to millimeters thick) of the nanocomposite by pressing the viscous melt onto a conductive substrate [such as Al or In-tin oxide (ITO) conducting glass] under N_2 and allowing it to cool to

Central Research and Development, Du Pont Experimental Station, Post Office Box 80356, Wilmington, DE 19880, USA.

*To whom correspondence should be addressed.

a deep red-orange to black material.

X-ray diffraction patterns of 50% by weight BiI_3 -nylon-11 and 75% by weight BiI_3 -nylon-11 prepared by the above method were obtained. For the 50% BiI_3 -nylon-11 sample, we observed only broad background scattering without any significant signals attributable to BiI_3 crystallites (Fig. 1A). We have established that it is possible to detect $\sim 16 \text{ \AA}$ CdS nanoclusters in a 1% by volume concentration in a polymer film a few micrometers thick (17). Because BiI_3 is much heavier than CdS and our sample was 500 \mu m thick, the detection sensitivity of the BiI_3 -nylon-11 should be even higher. Any BiI_3 crystallites larger than $\sim 15 \text{ \AA}$ with a concentration of $\geq 1\%$ by volume would have been easily detected. The absence of any BiI_3 x-ray diffraction peaks in the 50% by weight BiI_3 -nylon-11 sample therefore indicates that it can be identified as a true nanocomposite, with an upper limit of $\sim 15 \text{ \AA}$ on the domain size of the majority of the BiI_3 crystallites.

Although bulk BiI_3 is black, the 50% by weight BiI_3 -nylon-11 composite is orange-red and transparent. Both the color and the transparency indicate that BiI_3 is finely dispersed. The absorption spectrum of the composite shows a peak at 497 nm , which is blue-shifted from the direct band gap, E_g , of bulk BiI_3 located at 654 nm (Fig. 2). Also plotted for comparison in Fig. 2 is the spectrum of BiI_3 dissolved in N,N -dimethylformamide (DMF) solution [assigned to the BiI_3 -DMF molecular adducts (16)], which shows an absorption peak at 406 nm . Examination of the sample with transmission electron microscopy revealed a small percentage of BiI_3 nanocrystallites from 2 to 5 nm in size. However, most of the BiI_3 , which constitutes $\sim 14\%$ by volume of the sample, is not visible, as expected if BiI_3 is finely dispersed in nylon and if the domain sizes are very small.

As the concentration of BiI_3 was increased to 75% by weight, diffraction peaks attributable to BiI_3 crystallites appeared (Fig. 1B). In this case, the sample appeared clear and homogeneous in the molten state, but, after cooling, micrometer-sized, hexagonal BiI_3 crystallites could be clearly observed with an optical microscope. It should be possible to control the kinetics or use capping chemistry (1-8) to reduce the BiI_3 crystallite size at 75% by weight and higher concentrations. We focused our x-ray photoconductivity study on the 50% by weight BiI_3 -nylon-11 sample.

X-ray photoconductivity was characterized by the standard x-ray-induced discharge method (10, 13). An x-ray photoconductive film was cast onto a conductive substrate (for example, Al or ITO glass) by spin-coating or

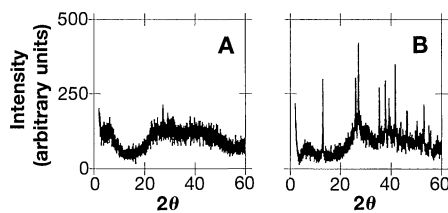


Fig. 1. X-ray diffraction of (A) 50% by weight BiI_3 -nylon-11 and (B) 75% by weight BiI_3 -nylon-11 with $\text{Cu } \alpha$ radiation; θ is the angle of incidence of the x-ray beam.

thermal pressing. The films used here typically had a thickness of several hundred micrometers. The surface of the film was then charged by a corona charger (Monroe Electronics model 152A Coronatrol). The amount of charge on the film was measured by an electrostatic voltmeter (Monroe Electronics model 244). Upon exposure to x-rays, electrons and holes are generated in the film, and these migrate to the film surface to discharge. The discharge rate correlates with the charge generation efficiency (10, 13, 14), and the completeness of the discharge indicates the absence of carrier traps. All of the data were taken with a Bennett x-ray unit (Copiagne, New York) equipped with a Mo target running at 28 kV, 100 mA, in a long filament mode. The output x-rays were further attenuated by Al disks 0.8 mm thick. The effective x-ray photon energy with the Al filter was 17.4 keV, based on the known absorption coefficient of Al. A high-quality, $300\text{-}\mu\text{m}$ -thick Se film on ITO glass was used as a reference.

X-ray-induced discharge curves of a 50% by weight BiI_3 -nylon-11 film $550 \text{ }\mu\text{m}$ thick were compared with those of a $300\text{-}\mu\text{m}$ Se film, both with positive charging (Fig. 3). The BiI_3 -nylon-11 film could be charged up to $\sim 10^5 \text{ V cm}^{-1}$ (limited by the corona supply), which indicates its good dielectric strength. In the absence of x-rays, the dark decay is slow even under such high fields (Fig. 3). These superior

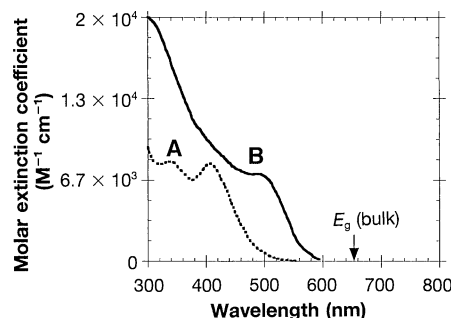


Fig. 2. The absorption spectra of (curve A) BiI_3 dissolved in DMF and of (curve B) the 50% by weight BiI_3 -nylon-11 nanocomposite. The bulk band gap, E_g , of BiI_3 is marked by the arrow at 654 nm .

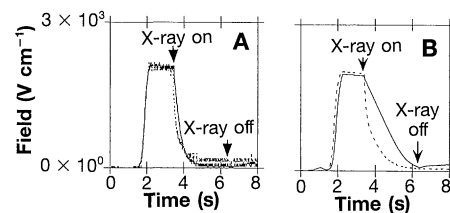


Fig. 3. X-ray-induced discharge curves of a $550\text{-}\mu\text{m}$ 50% by weight BiI_3 -nylon-11 film (solid lines) and a $300\text{-}\mu\text{m}$ Se film (dotted lines) at (A) $\sim 2 \times 10^3 \text{ V cm}^{-1}$ and (B) $2 \times 10^4 \text{ V cm}^{-1}$.

dielectric properties cannot be achieved with BiI_3 alone but are expected from polymers. With x-ray irradiation, the BiI_3 -nylon-11 sample showed fast and complete discharge (Fig. 3). The discharge curves are linear over their major portions. At low field, its discharge rate is comparable to that of Se (Fig. 3A). At higher field, the discharge rate of the composite is slower than that of Se (Fig. 3B).

The field dependences of the discharge rate (the initial slope of the discharge curve) for these materials were also compared (Fig. 4). Below $\sim 6 \times 10^3 \text{ V cm}^{-1}$, the discharge rate of the BiI_3 -nylon-11 sample was comparable to that of Se (Fig. 4A). At higher fields, the discharge rate of the sample levels off, whereas that of Se continues to increase. The initial discharge rate correlates with the charge generation efficiency (10, 13, 14), and therefore we attribute the field dependence to electron hole recombination within the "spurs" or "blobs" (regions where the electrons and holes are concentrated) (18). Evidently, an applied field of $\sim 6 \times 10^3 \text{ V cm}^{-1}$ is sufficient to overcome this electron hole recombination process for 50% by weight BiI_3 -nylon-11, although larger fields are needed for Se. The 50% by weight BiI_3 -nylon-11 material is also a good x-ray photoconductor with negative charging—that is, it is capable of transporting electrons (Fig. 4B). As in the case of positive charging, at fields smaller than $\sim 6 \times 10^3 \text{ V cm}^{-1}$, the discharge rates are comparable to those of Se, whereas they level off with larger fields.

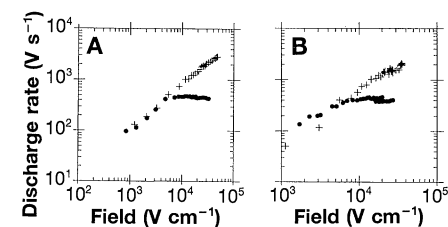


Fig. 4. Field dependence of the initial slopes of the discharge curves for 50% by weight BiI_3 -nylon-11 (\bullet) and Se (+) samples with (A) positive charging and (B) negative charging.

Nylon-11 itself is not a carrier-transporting material. The observed ability of BiI_3 -nylon-11 nanocomposites to transport both electrons and holes is the result of the presence of BiI_3 . The ability to sustain high field and the low dark conductivity (Fig. 3) show that the composite is not an ionic solid. The conduction mechanism is electronic rather than ionic. At a 50% by weight loading level (~14% by volume), the conduction pathway can be established upon the percolation of BiI_3 domains. Electrons and holes can then hop along the BiI_3 domains. The transport mechanism should be very similar to the disorder transport model established for amine-doped polymers (19).

The leveling-off of the discharge rate with large fields (Figs. 3 and 4) results from the limited amount of x-ray-absorbing BiI_3 present in the composites. This can limit not only the number of x-ray absorption centers per unit volume but also the charge generation efficiency. After x-ray absorption by BiI_3 , the electron-hole pairs are generated mostly in the polymer matrix (~86% by volume), which has a large band gap and which may have lower charge generation efficiency [it has been shown that the electron-hole generation efficiency is inversely proportional to E_g (20)]. Clearly, a more efficient x-ray photoconductor will result if the BiI_3 concentration in the composite can be increased while its fine dispersion is maintained. As pointed out in Fig. 1B, simple cooling of a melt with 75% by weight BiI_3 results in micrometer-sized BiI_3 crystallites. We have verified that the charge generation efficiency of the 75% sample is reduced as compared to that of the 50% sample. Therefore, techniques need to be developed to limit the growth of BiI_3 crystallites to the nanosize regime. Many such techniques have been demonstrated in solution phase (1-8) and could be extended to this problem.

Other inorganic-polymer combinations could also be explored. Our search has led us to several additional x-ray photoconductive nanocomposites with inorganic compounds such as PbI_2 and HgI_2 and polymers such as *N*-polyvinylcarbazole and polystyrene. The threshold concentrations for the formation of large inorganic crystallites are lower for these composites than for BiI_3 , because of the weaker interaction between the inorganic compounds and the polymer. Maximal interaction between the inorganic compounds and polymers therefore seems to be an important design element. Alternatively, one could synthetically attach strong x-ray-absorbing inorganic nanoclusters directly to the polymers.

REFERENCES AND NOTES

- M. L. Steigerwald and L. E. Brus, *Acc. Chem. Res.* **23**, 183 (1990).
- Y. Wang and N. Herron, *J. Phys. Chem.* **95**, 525 (1991).
- Y. Wang, *Adv. Photochem.* **19**, 179 (1995).
- H. Weller, *Angew. Chem.* **105**, 43 (1993).
- H. Gleiter, *Adv. Mater.* **4**, 474 (1992).
- J. H. Fendler, *Membrane-Mimetic Approach to Advanced Materials* (Advances in Polymer Science Series, vol. 113, Springer-Verlag, Berlin, 1994).
- C. B. Murray, D. J. Norris, M. G. Bawendi, *J. Am. Chem. Soc.* **115**, 8706 (1993).
- S. H. Tolbert and A. P. Alivisatos, *Science* **265**, 373 (1994).
- L. K. Wagner, P. Narayana, R. C. Murry Jr., in *Imaging Processes and Materials*, J. Sturge, V. Walworth, A. Shepp, Eds. (Van Nostrand Reinhold, New York, 1989), p. 497.
- J. A. Rowlands, D. M. Hunter, N. Araj, *Med. Phys.* **18**, 421 (1991).
- W. Hillen, U. Schiebel, T. Zaengel, in *Medical Imaging II*, R. H. Schneider and S. J. Dwyer, Eds. [SPIE **914**, 253 (1988)].
- W. Zhao and J. A. Rowlands, in *Extended Abstracts of the Electrochemical Society Meeting*, Toronto, Ontario, Canada, 11 to 16 October 1992 (Electrochemical Society, Pennington, NJ, 1992), vol. 92-2, p. 791.
- J. L. Donovan, *J. Appl. Phys.* **50**, 6500 (1979).
- Y. Wang, in *Kirk-Othmer Encyclopedia of Chemical Technology* (Wiley, New York, ed. 4, 1996), p. 837.
- J. Trotter and T. Zobel, *Z. Kristallogr.* **123**, 67 (1966).
- W. Clegg et al., *J. Chem. Soc. Dalton Trans.* **1993**, 2579 (1993).
- Y. Wang and N. Herron, *Chem. Phys. Lett.* **200**, 71 (1992); Y. Wang et al., *J. Chem. Phys.* **92**, 6927 (1990).
- J. W. T. Spinks and R. J. Woods, *An Introduction to Radiation Chemistry* (Wiley, New York, 1976).
- H. Bässler, *Phys. Status Solidi B* **175**, 15 (1993).
- R. C. Alig and S. Bloom, *Phys. Rev. Lett.* **35**, 1522 (1975).
- We thank J. B. Jensen and S. Harvey for technical assistance and R. Li for electron microscopy. This is Du Pont Co. contribution 7355.

4 March 1996; accepted 10 June 1996

A Fluted Point from the Uptar Site, Northeastern Siberia

Maureen L. King* and Sergei B. Slobodin

Lanceolate bifacial points, including one fluted specimen, have been collected from beneath an early Holocene tephra at the Uptar site, northeastern Siberia. Thus, the technology associated with the well-known Paleoindian tradition was not confined to the Americas. The Uptar collection does not compare readily with other Beringian complexes and demonstrates that there is greater diversity in the archaeological record of northeastern Siberia than traditional colonization models imply.

During the Pleistocene epoch far northwestern North America was the eastern part of a vast subcontinent, named Beringia, that connected the Old and New Worlds. The Bering Land Bridge provided a major pathway for the exchange of plants and animals as well as a corridor for the entry of early peoples to North America (1). By about 11,000 to 10,000 radiocarbon years before the present (years B.P.), the land bridge was submerged and the western and eastern remnants of Beringia again became two separate geographic regions (2). Presuming an overland entry for early colonizers of the Americas, the western remnant of Beringia (northeastern Siberia) was the point of departure.

The earliest firmly documented tradition in the New World, the Paleoindian tradition (11,200 to 8500 years B.P.), begins with a distinctive series of fluted lanceolate

bifacial points. Data from northeastern Siberia are too few to indicate much about the colonization of Beringia (3); however, the earliest firmly documented tradition in eastern Siberia (the Upper Paleolithic Duktai culture from the Aldan basin, 35,000 to 10,000 years B.P.) (4) is thought (5-7) to bear little resemblance to Paleoindian traditions. The origin of fluting has been controversial and involves a debate not only about the source of a distinctive technology, but also about the peopling of the Americas (8).

Here, we describe excavations at the Uptar site in Magadan Oblast, northeastern Siberia (Fig. 1), including a stone tool assemblage with lanceolate bifaces and a fluted point. The Uptar site is 40 km north of Magadan in a tectonic basin bordered to the north by the Kolyma Upland and to the south by the Okhotsk Sea. At ~160 m above sea level, the site is on a fluvial terrace 4 to 5 m above the modern floodplain of the Uptar River, a tributary of the Arman River. The site was discovered in 1984, and subsequent surface collection and excavation have taken place over an area of 32 m² (9).

A 2- to 10-cm-thick deposit of the

M. L. King, Department of Anthropology, University of Washington, and Desert Research Institute, Quaternary Sciences Center, Post Office Box 19040, Las Vegas, NV 89132, USA.

S. B. Slobodin, Department of Education, Apartment 19, 14 Dzerzhinsky Street, Magadan, 68500 Russia.

* To whom correspondence should be addressed. E-mail: maureen@sns.c.dri.edu.